Green Synthesis and Characterization of Silver Nanoparticles Using *Crotalaria spectabilis* Roth.

Aradhana[#1] and Mukesh Kumar*

Department of Botany and Microbiology, Gurukula Kangri (Deemed to be University), Haridwar-249404, Uttarakhand, India

1st Author: Aradhana, giriaradhana105@gmail.com,

2nd Author: Mukesh Kumar, mukesh.kumar@gkv.ac.in,

*Corresponding author, Email: mukesh.kumar@gkv.ac.in

Abstract

The present study reports the eco-friendly synthesis of silver nanoparticles (AgNPs) using the aqueous leaf extract of *Crotalaria spectabilis* as both a reducing and stabilizing agent. Phytochemicals present in the extract facilitated the rapid reduction of Ag^{+} ions, resulting in the formation of stable AgNPs. To elucidate the functional groups involved in this process, Fourier-transform infrared spectroscopy (FTIR) analysis was performed, confirming the role of biomolecules in capping and stabilization of the nanoparticles. Additional characterization techniques, including X-ray diffraction (XRD), field emission scanning electron microscopy (FESEM), and energy-dispersive X-ray spectroscopy (EDX), were employed. XRD analysis revealed a crystallite size of 24.6 nm, while FESEM confirmed uniform morphology and nanoscale dimensions. EDX analysis validated the elemental composition of silver. Phytochemicals such as polyphenols and flavonoids were identified as key reducing agents. The synthesized AgNPs exhibited excellent stability, underscoring their potential for diverse applications. Overall, this study demonstrates *Crotalaria spectabilis* as a promising plant source for sustainable and cost-effective nanoparticle production, contributing to the advancement of green nanotechnology.

Keywords: Nanoparticles, Green Nanotechnology, Nanoparticles, Phytochemicals, stabilizing agent, XRD.

I. INTRODUCTION

The concept of nanotechnology was first introduced by Richard Feynman in 1959 and later defined more precisely by Norio Taniguchi in 1974. A major practical breakthrough came with the invention of the Scanning Tunneling Microscope in 1981, which enabled direct manipulation and observation at the atomic scale. Since then, nanotechnology has evolved into one of the most transformative scientific domains of the 21st century, driving advancements in medicine, agriculture, electronics, materials science, and environmental engineering [1]. Nanotechnology is broadly described as the manipulation of matter at the nanoscale (1–100 nm) [2]. At this scale, materials exhibit unique optical, electrical, thermal, and catalytic behaviors, largely attributed to quantum effects and high surface-to-volume ratios [3]. Among the various nanomaterials, metallic nanoparticles, particularly silver nanoparticles, have drawn considerable attention as a result of their strong antimicrobial nature, biocompatibility, and catalytic versatility [4]. These properties have facilitated their application in biomedical devices, diagnostics, targeted drug delivery, water treatment, food packaging, agriculture, and environmental remediation [5]. Importantly, the performance and functionality of AgNPs are highly dependent on factors such as particle size, shape, and surface chemistry, underscoring the need for controlled synthesis strategies [6].

Conventional chemical and physical approaches to nanoparticle synthesis, while effective, often rely on toxic reagents, high energy consumption, and expensive instrumentation, raising significant environmental and safety concerns [7]. As a sustainable alternative, green synthesis using biological resources has gained increasing attention. Among these, plant-mediated synthesis is particularly advantageous due to the easy availability of

plant extracts, their simple preparation, and the abundance of phytochemicals with inherent reducing and stabilizing capabilities [8]. Bioactive compounds such as phenols, flavonoids, terpenoids, and proteins not only facilitate the formation of metallic silver (Ag^0) and the reduction of silver ions (Ag^+), but also prevent aggregation, thereby enhancing the stability of the nanoparticles [9]. The morphology and size of the resulting nanoparticles are strongly influenced by parameters such as pH and temperature, making optimization crucial for achieving monodispersity [10]. Characterization techniques are essential to confirm successful green synthesis and to evaluate nanoparticle properties. UV–Visible spectroscopy detects nanoparticle formation through surface plasmon resonance, FTIR identifies functional groups involved in capping, XRD provides information on crystallinity, and SEM/TEM reveal particle morphology and size distribution [7]. Plant-mediated silver nanoparticles (AgNPs) have demonstrated broad applicability across multiple sectors. In medicine, they function as antimicrobial coatings, wound-healing agents, and targeted drug delivery systems. In agriculture, they enhance crop productivity and serve as eco-friendly pesticides. In environmental science, they contribute to water purification and pollutant monitoring. Beyond these, their integration into packaging, cosmetics, and biosensors highlights their versatility and growing industrial relevance [11].

II. Materials and Methods

In order to synthesize silver nanoparticles from plant extract, first of all, plant material collection was done. Plant material collection was conducted in compliance with national and international ethical guidelines. In this study, *Crotalaria spectabilis* was chosen as the plant material for the plant-mediated synthesis of silver nanoparticles. The selected species, *Crotalaria spectabilis* Roth. (commonly known as the showy rattlebox or showy rattlepod), is neither endangered nor sourced from wild habitats; instead, it is widely cultivated across India and readily available locally. Furthermore, the Literature review suggests that there is high polyphenolic content that can enhance its potential as an efficient reducing agent for nanoparticle synthesis.

Collection of Plant Materials

Healthy, disease-free leaves of *Crotalaria spectabilis* Roth were collected in September 2024 from the Department of Botany and Microbiology, Gurukula Kangri (Deemed to be University), Haridwar, India. The plant material was taxonomically identified and authenticated by the Botanical Survey of India (BSI), Northern Regional Centre, Dehradun, with accession number 1654. A herbarium specimen of *C. spectabilis* has been prepared and deposited in the Department of Botany and Microbiology, Gurukula Kangri (Deemed to be University), Haridwar, for future reference.

Fig. 1 *Crotalaria spectabilis* plant in the field

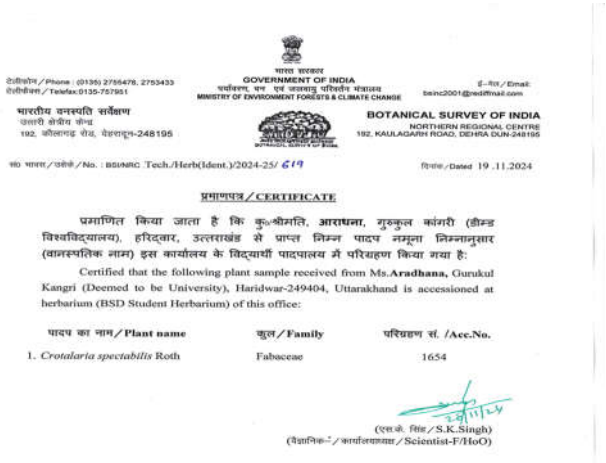

GOVERNMENT OF INDIA
MINISTRY OF ENVIRONMENT FORESTS & CLIMATE CHANGE
BOTANICAL SURVEY OF INDIA
NORTHERN REGIONAL CENTRE
192, KAULAGARH ROAD, DEHRA DUN-248195

No. : BSI/NRC /Tech./Herb(Ident.)/2024-25/ 619 Dated 19 .11.2024

प्रमाणपत्र / CERTIFICATE

प्रमाणित किया जाता है कि कु.श्रीमति, आराधना, गुरुकुल कांगरी (डीम्ड विश्वविद्यालय), हरिद्वार, उत्तराखंड से प्राप्त निम्न पादप नमूना निम्नानुसार (वानस्पतिक नाम) इस कार्यालय के विद्यार्थी पादपालय में परिग्रहण किया गया है:

Certified that the following plant sample received from Ms.**Aradhana,** Gurukul Kangri (Deemed to be University), Haridwar-249404, Uttarakhand is accessioned at herbarium (BSD Student Herbarium) of this office:

पादप का नाम / Plant name	कुल / Family	परिग्रहण सं. /Acc.No.
1. *Crotalaria spectabilis* Roth	Fabaceae	1654

(एस.के. सिंह / S.K.Singh)
(वैज्ञानिक-F / कार्यालयाध्यक्ष / Scientist-F/HoO)

Fig. 2 Authentication certificate of the experimental plant.

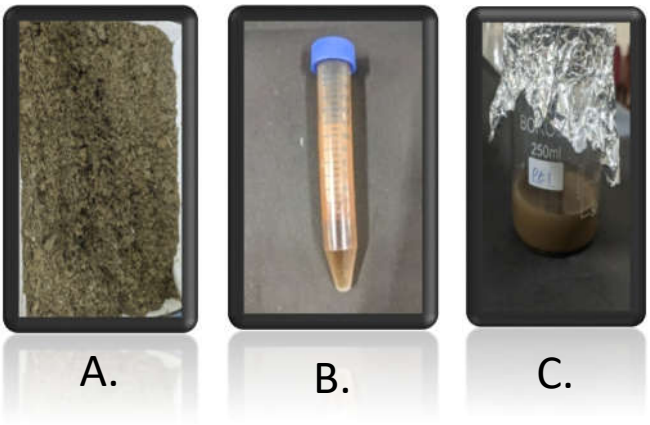

Fig. 3 Protocol for AgNPs Synthesis A. Plant Leaves Powder B-C. Production of Brown color showing nanoparticle synthesis

Protocol for Plant Extraction Procedure

Fresh leaves of *Crotalaria spectabilis* were rinsed using tap water and subsequently with distilled water, air-dried, and finely chopped. The leaves were then shade-dried, ground into a fine powder, and stored for subsequent extraction. Crude plant extract was prepared following standard phytochemical protocols. The selection of an extraction technique generally depends on factors such as plant texture, moisture content, and the chemical nature of the target compounds. In this study, Soxhlet extraction was performed using methanol and ethanol as solvents. These solvents were chosen due to their broad solubility range for organic compounds and their relatively low boiling points, which facilitate efficient extraction and easy solvent recovery.

Soxhlet Extraction

Approximately 100 g of dried plant powder was placed in the thimble chamber of a Soxhlet apparatus, and extraction was performed separately using 1500 mL of ethanol and methanol as solvents [12]. During the process, solvent vapors passed through the sample chamber, condensed in the condenser, and continuously percolated through the plant material. Once the siphon arm is filled, the solvent drained back into the boiling flask, allowing the cycle to repeat. Extraction was carried out for 48 hours. The obtained extracts were concentrated by evaporating the solvent at 70 °C for 8 hours, followed by drying and conversion into a gel form. The final extracts were stored at room temperature until further analysis by GC–MS [13].

Phytochemical Screening using GC-MS

The crude extract was filtered to remove insoluble residues, resulting in a clear solution. The methanolic and ethanolic extracts of *Crotalaria spectabilis* were then analyzed for volatile compounds using gas chromatography–mass spectrometry (GC–MS). A Shimadzu QP 2010 Ultra GC–MS system (Shimadzu, Japan) fitted with an HP-5 column (30 m × 0.25 mm × 0.25 µm film thickness) was used for the analysis. The spectrometer was operated with a mass range of 35–750 amu. The oven temperature was programmed up to 310 °C, while the detector temperature was maintained at 260 °C. Helium was used as the carrier gas at a flow rate of 1 mL/min. For detection, an electron ionization source with an ionization energy of +70 eV was employed. The retention time (RT) was recorded as the interval between sample injection and compound elution [14].

Synthesis of Silver Nanoparticles (AgNPs)

A 1 mM aqueous solution of silver nitrate ($AgNO_3$) was made in 250 mL Erlenmeyer flasks, followed by the addition of plant extract filtrate to reduce Ag^+ ions to metallic silver (Ag^0) nanoparticles. The mixture was then subjected to microwave irradiation at 300 W for 4 min in intermittent cycles to control pressure build-up. During the process, formed nanoparticles were visually monitored by a distinct colour change from pale yellow to yellowish-brown, reddish-brown, and finally colloidal brown. All reactions were conducted in the dark to avoid photoactivation of $AgNO_3$, and appropriate controls were maintained throughout the experiments. Complete conversion of Ag^+ to metallic Ag^0 was confirmed by the colour change to colloidal brown. After irradiation, the solution was cooled to room temperature and stored undisturbed for 24 h to achieve full bio-reduction and stabilization. The reaction mixture was subsequently centrifuged at 4000 rpm for 30 min at 24 °C [15].

Mechanism of Plant-Mediated Nanoparticle Formation

The bio-reduction of Ag^+ ions by plant extracts is primarily driven by phytochemicals such as terpenoids, flavonoids, alkaloids, phenols, tannins, and proteins. These molecules interact electrostatically with silver ions, reducing them to

metallic silver nuclei. As the reaction progresses, additional silver ions deposit onto these nuclei, promoting controlled nanoparticle growth. This environmentally friendly approach negates the need for harmful chemicals and supports the principles of green chemistry by being cost-effective, sustainable, and environmentally safe [16].

Characterization of Silver Nanoparticles

The successful synthesis of silver nanoparticles (AgNPs) was validated using multiple analytical techniques. Field Emission Scanning Electron Microscopy (FESEM), combined with Energy-Dispersive X-ray (EDX) analysis, delivered valuable insights into surface morphology, particle size distribution, and elemental composition, thereby verifying the presence of silver. X-ray Diffraction (XRD) analysis displayed sharp diffraction peaks consistent with the crystalline structure of AgNPs, further confirming their well-defined nature. Additionally, Fourier Transform Infrared Spectroscopy (FTIR) was employed to identify functional groups derived from phytochemicals in the plant extract, which played a dual role in facilitating silver ion reduction and nanoparticles stabilization/capping [17].

III. RESULT

X-ray Diffraction (XRD)

This X-ray Diffraction (XRD) spectrum validates the synthesis of AgNPs. XRD analysis was performed to determine the crystalline structure, phase purity, and average crystallite size of the nanoparticles. Distinct diffraction peaks were observed at 2θ values of 28.14°, 32.52°, 38.41°, 46.55°, and 57.79°. The prominent peak at 38.41° corresponds to the (111) plane of face-centered cubic (fcc) silver, which serves as the characteristic fingerprint of crystalline AgNPs. The additional peaks can be indexed to the (200), (220), and (311) planes of fcc silver, consistent with the standard JCPDS card no. 04-0783. The sharpness and intensity of these peaks confirm the high crystallinity of the synthesized nanoparticles. Overall, the XRD spectrum validates the crystalline nature of biosynthesized AgNPs, with diffraction peaks corresponding to the standard fcc structure of silver. The absence of noticeable impurity peaks further confirms their phase purity and structural stability. Debye-Scherrer equation states that $D = k\lambda/\beta \cos\theta$, where D is particle size (nm), k is a constant of 0.94, λ is the wavelength for the X-ray source used at (0.1541nm), β is the full width at half maximum (FWHM), and θ is the half diffraction angle or Bragg angle (degree°). Average crystal size was found out to be 24.72 nm, which is relatively close to previous findings [18].

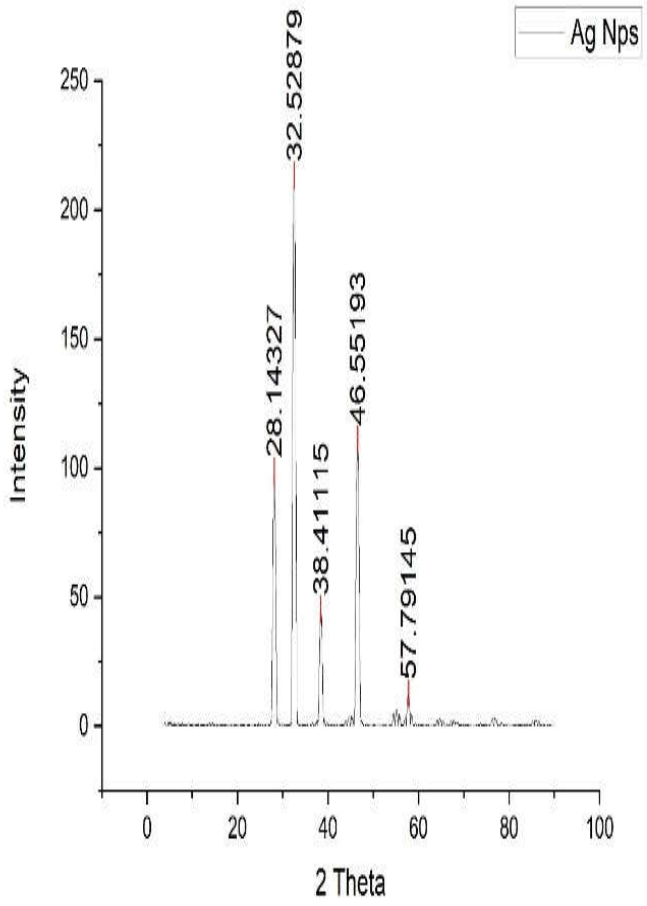

Fig. 4 X-ray diffraction (XRD) pattern of biosynthesized Ag-NPs

Table. I Ag-NPs Average Size Calculation Using XRD

2θ (°)	θ (°)	cosθ	FWHM β (°)	β (rad)	λ (Å)	D (nm)	d (Å)	hkl	a (Å)
28.14	14.07	0.970	0.36	0.00629	1.5406	23.40	3.1682	111	5.49
32.53	16.265	0.958	0.32	0.00559	1.5406	27.58	2.7504	200	5.50
38.41	19.205	0.945	0.35	0.00611	1.5406	24.74	2.3416	220	5.52
46.55	23.275	0.920	0.38	0.00663	1.5406	24.02	1.9493	311	5.51
57.79	28.895	0.878	0.40	0.00698	1.5406	23.88	1.5941	222	5.52

here,

2θ (°): Measured diffraction angle from XRD, **θ (°)**: Bragg angle (2θ ÷ 2), **cos θ**: Cosine of Bragg angle, used in Debye–Scherrer, **FWHM β (°)**: Full width at half maximum of the peak (degrees), **β (rad)**: FWHM converted to radians (β×π/180β × π/180β×π/180), **λ (Å)**: X-ray wavelength, **D (nm)**: Crystallite size calculated using Debye–Scherrer equation, **d (Å)**: Interplanar spacing (from Bragg's law), **hkl**: Miller indices of the plane, **a (Å)**: Lattice constant

EDX Analysis

The EDX spectrum of the synthesized sample confirmed the successful formation of silver nanoparticles (AgNPs), as evidenced by a strong and distinct characteristic peak at approximately 3 keV, which is a well-established signature of silver. An additional minor silver peak in the low-energy region (~0.2 keV) further verified the predominance of silver in the sample. Minor peaks corresponding to oxygen (~0.5 keV) and chlorine (~2.6 keV) were also detected, likely arising from surface oxidation of the nanoparticles, interactions with phytochemicals present in the plant extract, or residual ions from precursor salts and stabilizing agents. The clear dominance of silver peaks over other elemental signals confirmed that the nanoparticles were primarily composed of silver, thereby validating both the elemental purity and the successful biosynthesis of AgNPs [19].

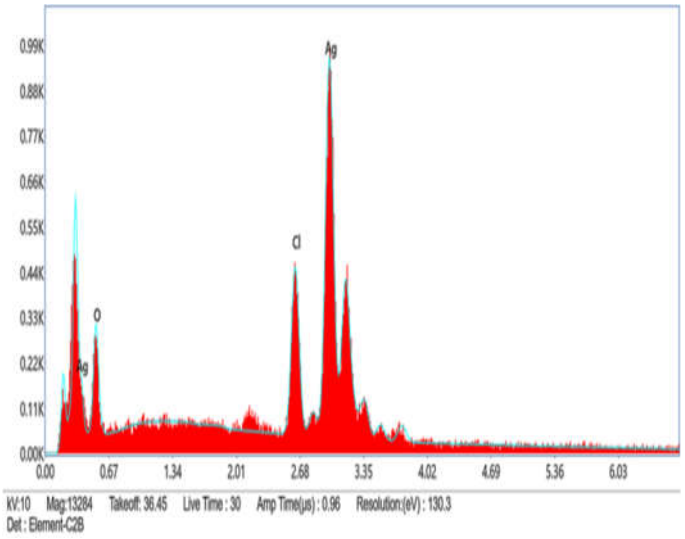

Fig. 5 EDX pattern of biosynthesized Ag-NPs

FTIR (Fourier Transform Infrared)

The FTIR (Fourier Transform Infrared) spectrum of the synthesized silver nanoparticles (AgNPs) was analyzed to identify the functional groups involved in their reduction, stabilization, and capping. The FTIR spectrum of the synthesized silver nanoparticles (AgNPs) exhibited several characteristic absorption bands corresponding to functional groups of plant-derived biomolecules responsible for their reduction and stabilization. A broad band at 3804.87 cm^{-1}

and 3258.14 cm^{-1} was attributed to O–H stretching vibrations of alcohols/phenols or N–H stretching of amines, suggesting the participation of hydroxyl and amine groups from plant metabolites as capping agents. The band at 2156.99 cm^{-1} corresponded to C≡C or C≡N stretching vibrations, indicating the possible existence of alkyne or nitrile groups. A strong absorption peak at 1608.34 cm^{-1} was assigned to C=O stretching (amide I band) or C=C stretching of aromatic compounds, signifying the role of proteins and polyphenolic compounds in nanoparticle stabilization. The band at 1341.25 cm^{-1} reflected C–N stretching vibrations of amines or amides, further supporting protein/alkaloid involvement. Similarly, the peak at 1208.18 cm^{-1} was associated with C–O stretching of alcohols, esters, or carboxylic acids, while the absorption at 1039.44 cm^{-1} indicated C–O–C stretching of polysaccharides or ethers. The band at 938.19 cm^{-1} corresponded to C–H bending or skeletal vibrations of biomolecules. The FTIR spectrum revealed the presence of diverse functional groups, including hydroxyl, amine, carbonyl, and C–O bonds, originating from phytochemicals such as phenols, flavonoids, proteins, and polysaccharides. These biomolecules play a dual role by mediating the bioreduction of silver ions ($Ag^{+} \rightarrow Ag^{0}$) and acting as stabilizing and capping agents, thereby enhancing the stability of the synthesized AgNPs. Peaks observed at 812.29 and 523.53 cm^{-1}, located within the fingerprint region, correspond to metal–oxygen or Ag–N bond vibrations, confirming the interaction between silver and the plant-derived biomolecules. Overall, the FTIR analysis substantiates that phenolic compounds, flavonoids, proteins, and polysaccharides are directly involved in the reduction of silver ions to metallic silver while simultaneously preventing nanoparticle aggregation through capping and stabilization [20].

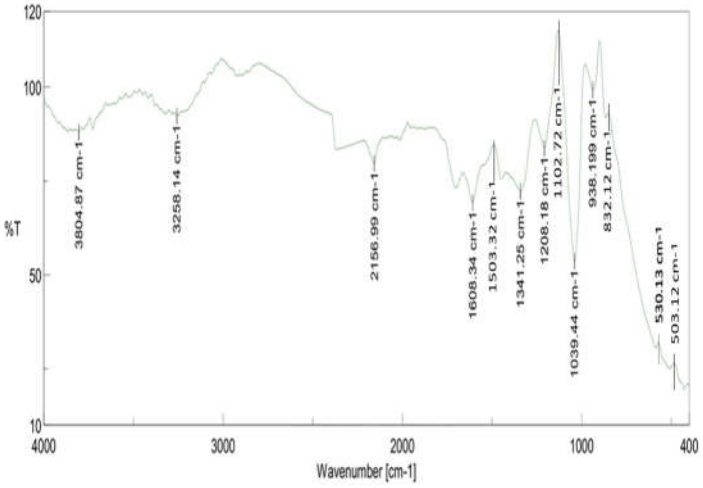

Fig.6 FTIR pattern of biosynthesized Ag-NPs

Field Emission Scanning Electron Microscopy (FESEM)

The Scanning Electron Microscopy (SEM) analysis was performed to examine the surface morphology, particle size, and aggregation behavior of the synthesized silver nanoparticles (AgNPs). The micrographs revealed predominantly spherical to quasi-spherical nanoparticles arranged densely and irregularly. Noticeable clustering and agglomeration were observed, which can be attributed to the high surface energy of the nanoparticles and their interactions with plant-derived capping biomolecules. Based on the magnification scales (5KX with a 2 µm bar and 20KX with a 500 nm bar), the particles were confirmed to fall within the nanometer range. Overall, SEM analysis validated the successful synthesis of AgNPs, exhibiting spherical morphology and aggregated clusters—a typical characteristic of biologically synthesized nanoparticles stabilized by phytochemicals [21].

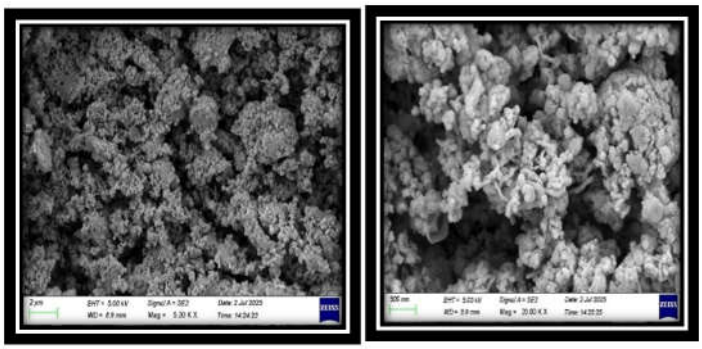

Fig. 7 FESEM image of green-synthesized silver nanoparticles

GC-MS Analysis

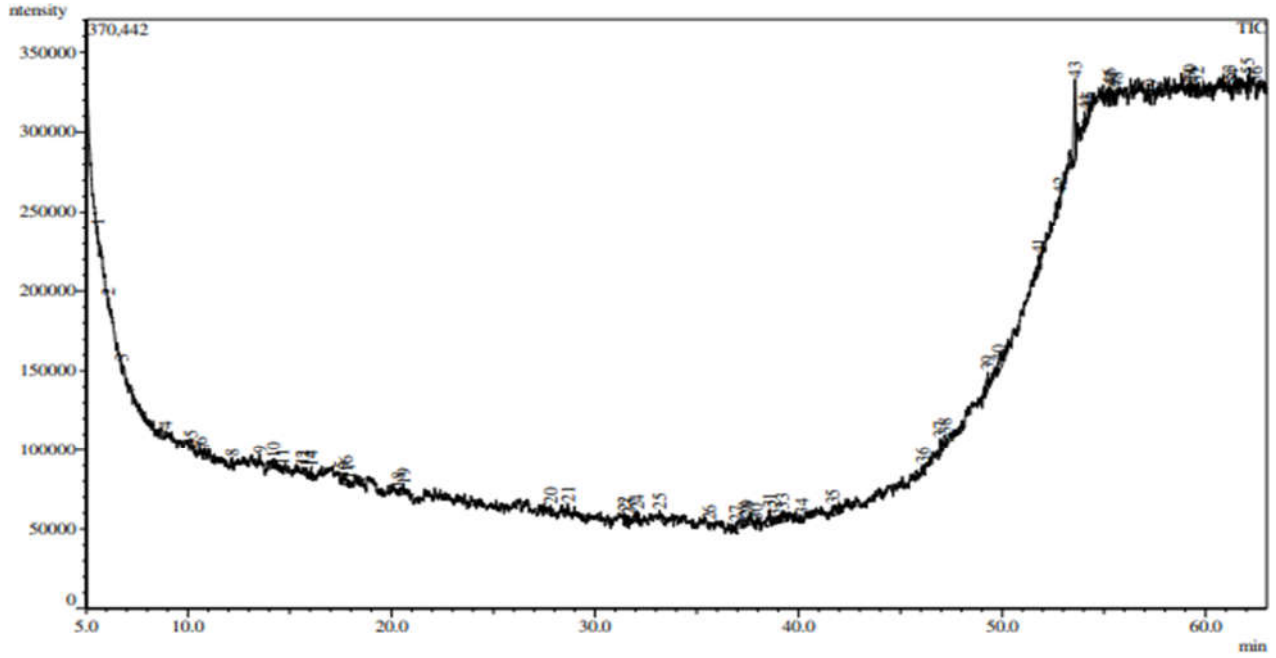

Fig. 8 Graphical representation of GC-MS of sample 6 extract

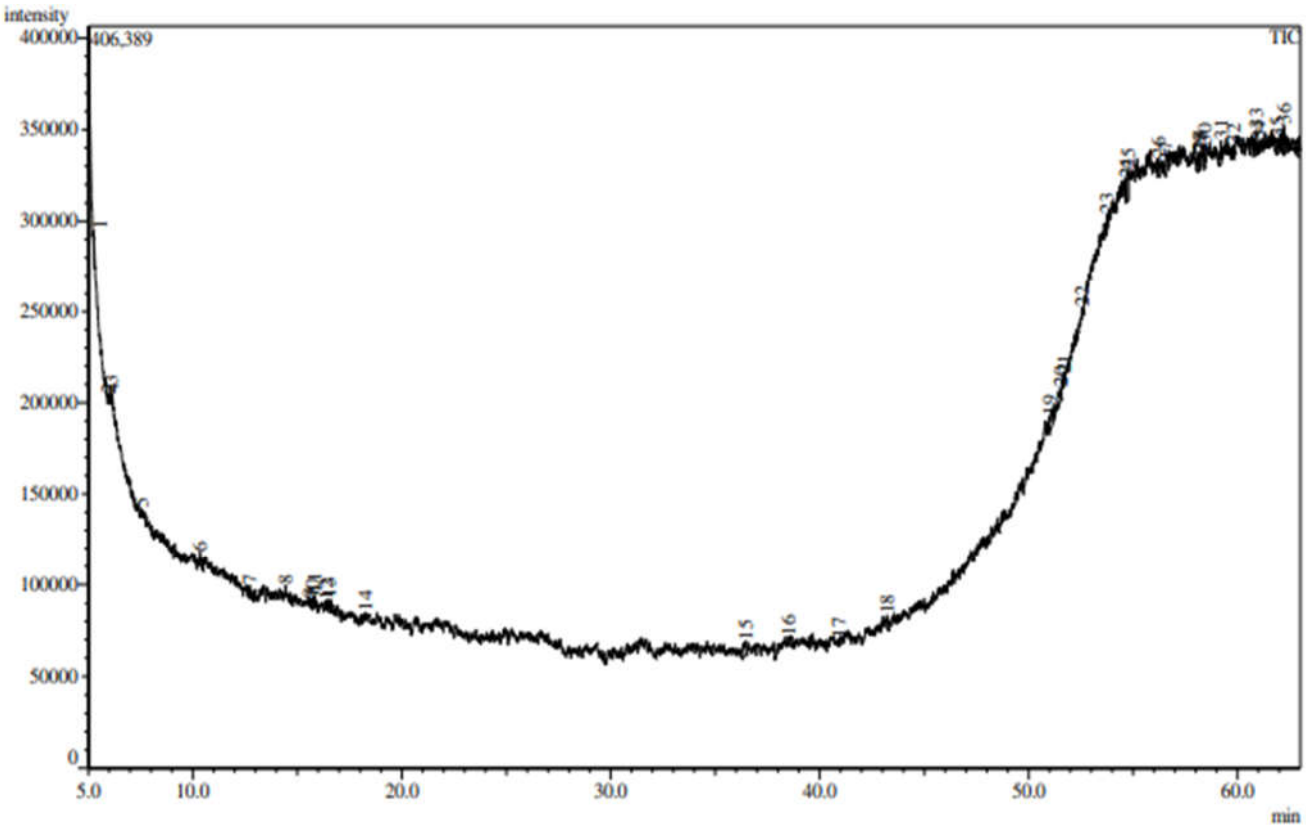

Fig. 9 Graphical representation of GC-MS of ethanolic extract

Table. II GC-MS Data Analysis of Methanolic Extract of *Crotalario spectabilis*

Peak	Rt*	Area%	Name	Molecular formula
1	5.543	0.64	Thiophene-3-ol, tetrahydro-, 1,1-dioxide	C4H8O3S
2	6.083	1.47	Cyclohexanone, 3-hydroxy-	C6H10O2
3	6.747	0.45	Benzo[b]1,4-dioxin, 2,3-dihydro-2-(1-benzylamino) ethyl-	C17H19NO2
4	8.883	0.27	2-Chloroprop-2-enamide	C3H4ClNO
5	10.159	2.54	O-Methylisourea	C2H6N2O
6	10.592	0.57	6-APDB	C11H15NO
7	10.733	2.69	Chlorodifluoroacetamide	C2H2ClF2NO
8	12.160	0.45	Ethene, (2-chloroethoxy)-	C4H7ClO
9	13.519	0.52	(S)-(+)-1-Cyclohexylethylamine	C8H17N
10	14.192	1.38	1-(5-Bicyclo[2.2.1]heptyl)ethylamine	C9H17N
11	14.633	0.26	Ethylamine, 1-(2-thenyl)-, hydrochloride	C7H11NS
12	15.625	1.58	Propylcarbamate	C4H9NO2
13	15.817	1.58	Ether, 2-chloro-1-methylethyl isopropyl	C6H13ClO
14	16.046	1.21	Benzeneethanamine, 4-fluoro-.alpha.-methyl-	C9H12FN
15	17.500	0.78	Acetic acid, [(aminocarbonyl)amino]oxo-	C3H4N2O4
16	17.762	3.38	Ethylamine, 1-(2-thenyl)-, hydrochloride	C6H9NS.ClH
17	17.892	0.49	Thiophene-3-ol, tetrahydro-, 1,1-dioxide	C4H8O2S
18	20.325	2.52	Formic acid, 2-methylpropyl ester	C5H10O2
19	20.594	0.41	N-[3,5-Dinitropyridin-2-yl]proline	C10H10N4O6
20	27.818	0.59	Dimethyl-(6-methyl-2-thioxo-[1,3,2]oxathiaphosphinan-2-yl)-amine	C6H14NOPS2
21	28.661	1.60	Thiophene-3-ol, tetrahydro-, 1,1-dioxide	C4H8O2S
22	31.442	1.45	Thiophene-3-ol, tetrahydro-, 1,1-dioxide	C4H8O2S
23	31.649	0.61	Propan-2-one, 1,1,1-trifluoro-3-dimethylhydrazono-3-(4-nitrophenyl)-	C11H10F3N3O3
24	32.068	0.56	Acetic acid, 2-(N-methyl-N-phosphonatomethyl)amino-	C4H10NO5P
25	33.168	2.83	Propanamide, N-methyl-2-amino-	C4H10N2O
26	35.588	0.37	Bromoamphetamine	C9H12BrN
27	36.923	2.13	Pterin-6-carboxylic acid	C7H5N5O3
28	37.342	1.26	5-Bromo-N,N-dimethyl-2H-1,2,4-triazole-3-carboxamide	C5H7BrN4O
29	37.492	0.96	Benzaldehyde, 2-nitro-, diaminomethylidenhydrazone	C8H9N5O2
30	37.909	0.32	2-Iodohiistidine	C6H8IN3O2
31	38.577	3.84	2-[2-Methyl-2-aminoethyl]benzofuran	C11H13NO
33	39.186	2.56	Acetamide, N-methyl-N-(2-phenylethyl)-	C11H15NO
34	40.142	0.51	Ethanone, 1-(4-pyridinyl)-, oxime	C7H8N2O
35	41.653	0.68	1,1'-(4-Methyl-1,3-phenylene)bis[3-(5-benzyl-1,3,4-thiadiazol-2-yl)urea]	C27H24N8O2S2
36	46.088	1.26	Pterin-6-carboxylic acid	C7H5N5O3
37	46.960	2.78	4(15)-Selinene-11,12-diol, methyl ether	C16H28O2
38	47.174	2.63	Cyclopropanetetradecanoic acid, 2-octyl-, methyl ester	C26H50O2
39	49.300	3.41	Benzylamine, 2-hydroxy-N,N-di-[2-aminoethyl]-	C11H19N3O

40	49.800	5.43	Imidazole, 2-amino-5-[(2-carboxy)vinyl]-	C6H7N3O2
41	51.803	3.55	5-Nitro-3-(trifluoromethyl)pyridin-2-amine, N-acetyl	C8H6F3N3O3
42	52.850	1.30	3,4-Dimethylbenzoic acid, tert-butyldimethylsilyl ester	C15H24O2Si
43	53.574	16.99	28-Norolean-17-en-3-one	C29H46O
44	54.058	0.96	3-Ethoxy-1,1,1,5,5,5-hexamethyl-3-(trimethylsiloxy)trisiloxane	C11H32O4Si4
45	54.233	1.51	6-Chloro-2-oxo-2H-chromene-3-carboxylic acid, O-TMS	C13H13ClO4Si
46	55.250	1.63	2,6-Lutidine 3,5-dichloro-4-dodecylthio-	C19H31Cl2NS
47	55.350	2.72	3-Isopropoxy-1,1,1,5,5,5-hexamethyl-3-(trimethylsiloxy)trisiloxane	C12H34O4Si4
48	55.575	1.16	Cyclotrisiloxane, hexamethyl-	C6H18O3Si3
49	57.292	0.80	Pentasiloxane, dodecamethyl-	C12H36O4Si5
50	59.218	0.63	2-tert-Butylphenol, trimethylsily ether	C13H22Osi
51	59.254	0.75	1,1,1,3,5,5,5-Heptamethyltrisiloxane	C7H21O2Si3
52	59.589	0.64	2,6-Lutidine 3,5-dichloro-4-dodecylthio-	C19H31Cl2NS
53	61.160	0.48	3-Ethoxy-1,1,1,5,5,5-hexamethyl-3-(trimethylsiloxy)trisiloxane	C11H32O4Si4
54	61.305	1.20	Pyridine, 1,2,3,6-tetrahydro-1-methyl-4-[4-chlorophenyl]-	C12H14ClN
55	62.068	2.18	3-Phenyl oxindole, BSTFA derivative	C17H19NOSi
56	62.517	2.21	1,2-Bis(trimethylsilyl)benzene	C12H22Si2

The phytochemical profile of the extract was determined using Gas Chromatography–Mass Spectrometry (GC–MS), which revealed the presence of a variety of bioactive compounds with potential biological activities. A total of 56 compounds were identified, among which the major constituents were 28-Norolean-17-en-3-one (16.99%), Imidazole, 2-amino-5-[(2-carboxy)vinyl]- (5.43%), 2-[2-Methyl-2-aminoethyl]benzofuran (3.84%), 5-Nitro-3-(trifluoromethyl)pyridin-2-amine, N-acetyl (3.55%), and Benzylamine, 2-hydroxy-N, N-di-[2-aminoethyl]- (3.41%). Several other compounds, including 4(15)-Selinene-11,12-diol, methyl ether (2.78%), Cyclopropanetetradecanoic acid, 2-octyl-, methyl ester (2.63%), 3-Isopropoxy-1,1,1,5,5,5-hexamethyl-3-(trimethylsiloxy) trisiloxane (2.72%), 3-Phenyl oxindole, BSTFA derivative (2.18%), and Pterin-6-carboxylic acid (2.13%), were also detected in notable proportions. The minor components (<2%) included various nitrogen, sulfur, halogen, and silicon derivatives, such as thiophene-3-ol, tetrahydro-,1,1-dioxide, chlorodifluoroacetamide, propylcarbamate, and trimethylsilyl derivatives, which may contribute synergistically to the overall biological functionality. The identification of these phytochemicals, particularly terpenoids, heterocyclic compounds, and phenolic derivatives, indicates that the extract is rich in bioactive molecules, supporting its potential application in nanoparticle synthesis, antimicrobial activity, and therapeutic applications.

Three major compounds stand out due to their significant peak area percentages. The most prominent compound is 28-Norolean-17-en-3-one, which holds the highest peak area percentage of 16.99%. Following this, Imidazole, 2-amino-5-[(2-carboxy) vinyl]- is the second major compound with an area percentage of 5.43%. The third key compound is Benzylamine, 2-hydroxy-N, N-di-[2-aminoethyl]-, which has a peak area percentage of 3.41%. These compounds are notable for their prevalence in the given dataset and likely play significant roles in the mixture analysed.

Table. III GC-MS Data Analysis of Ethanolic Extract of *Crotalario spectabilis*

Peak	Rt*	Area%	Name	Molecular formula
1	5.257	0.80	Ethane, 1-chloro-2-nitro-	C2H4ClNO2
2	5.958	0.95	Dimethyl Sulfoxide	C2H6OS
3	6.070	3.51	S-(2,2,2-Trifluoroethyl) methanesulfonothioate	C3H5F3O2S2
4	6.117	0.56	Methylthiophosphonamidic acid, S-methyl ester	C2H8NOPS
5	7.510	0.95	Ethene, (2-chloroethoxy)-	C4H7ClO
6	10.345	2.95	2-Iodohiistidine	C6H8IN3O2
7	12.724	2.06	Thiophene-3-ol, tetrahydro-, 1,1-dioxide	C4H8O3S
8	14.443	0.66	Acetic acid, [(aminocarbonyl)amino]oxo-	C3H4N2O4
9	15.567	1.57	Benzeneethanamine, 2,5-difluoro-.beta.,3,4-trihydroxy-N-methyl-	C9H11F2NO3
10	15.708	2.31	(Z)-1-Chloro-2-(methylsulfonyl)ethylene	C3H5ClO2S
11	15.808	1.57	3-Pentanone, dimethylhydrazone	C7H16N2
12	16.358	1.03	1,2-Propanediol, 3-chloro-	C3H7ClO2
13	16.508	3.17	2,2-Difluorobut-3-en-1-yl 2-fluoroethyl ether	C6H9F3O
14	18.256	0.49	2-Pyrrol2-[2-(2-chloro-ethoxy)-ethoxy]-ethoxymorpho-phenol	C12H17ClO4
15	36.448	6.32	D-erythro-Pentose, 2-deoxy-	C5H10O4
16	38.492	3.10	(.+/-.)-Phenylpropanolamine, trimethylsilyl ether	C12H21NOSi
17	40.908	2.98	1-Adamantanemethylamine, .alpha.-methyl-	C12H21N
18	43.225	1.99	1-(4-Acetamidoanilino)-3,7-dimethylbenzo[4,5]imidazo[1,2-a]pyridine-4-carbonitrile	C22H19N5O
19	50.992	7.54	Silane, trimethyl[5-methyl-2-(1-methylethyl)phenoxy]-	C13H22Osi
20	51.535	4.18	1,2-Bis(trimethylsilyl)benzene	C12H22Si2
21	51.692	1.40	Silicic acid, diethyl bis(trimethylsilyl) ester	C10H28O4Si3
22	52.542	1.49	2,4,6-Cycloheptatrien-1-one, 3,5-bis-trimethylsilyl-	C13H22OSi2
23	53.740	2.61	Benzene, 2-[(tert-butyldimethylsilyl)oxy]-1-isopropyl-4-methyl-	C16H28Osi
24	54.653	2.20	Cyclotetrasiloxane, octamethyl	C8H24O4Si4
25	54.769	8.47	Benzoic acid, 3-methyl-2-trimethylsilyloxy-, trimethylsilyl ester	C14H24O3Si2
26	56.200	2.71	3-Ethoxy-1,1,1,5,5,5-hexamethyl-3-(trimethylsiloxy)trisiloxane	C11H32O4Si4
27	56.550	0.93	1,2-Bis(trimethylsilyl)benzene	C12H22Si2
28	58.155	4.42	Trimethyl[4-(1,1,3,3,-tetramethylbutyl)phenoxy]silane	C17H30Osi
29	58.207	1.25	1,2-Bis(trimethylsilyl)benzene	C12H22Si2
30	58.426	3.18	7,7,9,9,11,11-Hexamethyl-3,6,8,10,12,15-hexaoxa-7,9,11-trisilaheptadecane	C14H36O6Si3
31	59.201	4.46	1,4-Bis(trimethylsilyl)benzene	C12H22Si2
32	59.808	1.47	3-Ethoxy-1,1,1,5,5,5-hexamethyl-3-(trimethylsiloxy)trisiloxane	C11H32O4Si4
33	60.905	4.03	Cyclodecasiloxane, eicosamethyl-	C20H60O10Si10

The GC–MS analysis of the plant extract identified a total of 36 compounds, reflecting a chemically diverse mixture comprising organic and organosilicon derivatives. The major constituents included Benzoic acid, 3-methyl-2-trimethylsilyloxy-, trimethylsilyl ester (8.47%), Silane, trimethyl[5-methyl-2-(1-methylethyl) phenoxy]- (7.54%), D-erythro-Pentose, 2-deoxy- (6.32%), and 1,4-Bis(trimethylsilyl)benzene (6.19%), which collectively accounted for the dominant fraction of the chromatogram. Other significant compounds were Trimethyl[4-(1,1,3,3-tetramethylbutyl) phenoxy] silane (4.42%), 1,2-Bis(trimethylsilyl)benzene (4.18%), and Cyclodecasiloxane, eicosamethyl- (4.03%), indicating a strong prevalence of silane- and siloxane-based derivatives. Moderate peaks were observed for nitrogenous and halogenated compounds, including 2,2-Difluorobut-3-en-1-yl 2-fluoroethyl ether (3.17%), 7,7,9,9,11,11-Hexamethyl-3,6,8,10,12,15-hexaoxa-7,9,11-trisilaheptadecane (3.18%), 1-Adamantanemethylamine, α-methyl- (2.98%), and 2-Iodohistidine (2.95%). In addition, minor constituents (<2%) such as dimethyl sulfoxide, ethyl chloroethoxy derivatives, and morpholine-based phenols were detected. Overall, the chemical profile indicates a predominance of silyl and siloxane derivatives, accompanied by heteroatom-containing bioactive molecules, which may contribute to antioxidant, antimicrobial, and material-related functionalities. Among the identified compounds, the three most abundant were Benzoic acid, 3-methyl-2-trimethylsilyloxy-, trimethylsilyl ester (8.47%), Silane, trimethyl[5-methyl-2-(1-methylethyl) phenoxy]- (7.54%), and 1,4-Bis(trimethylsilyl)benzene (6.32%), with benzoic acid derivative representing the highest peak area percentage.

IV. DISCUSSION

The successful synthesis of silver nanoparticles (AgNPs) using *Crotalaria spectabilis* leaf extract highlights the promise of plant-mediated green nanotechnology as an eco-friendly alternative to traditional chemical and physical methods. The study's outcomes clearly demonstrate the role of phytochemicals, particularly flavonoids and phenolics, in both the silver ions reduction and nanoparticles stabilization processes. XRD analysis validated the crystalline structure of AgNPs, with an average particle size of ~24.6 nm as estimated from the Debye–Scherrer equation. This size falls within the range reported for biosynthesized AgNPs from other plant systems, such as *Azadirachta indica* (22–30 nm) [22] and *Moringa oleifera* (16–25 nm) [23], demonstrating that *C. spectabilis* is equally effective in reducing and stabilizing silver nanoparticles.

FTIR spectra revealed hydroxyl, amine, and carbonyl functional groups, confirming their dual role as reducing and capping agents. These results align with earlier studies demonstrating that phytochemicals act simultaneously as bioreductants and surface modifiers, thereby enhancing nanoparticle stability [15]. SEM and EDX analyses further supported these observations, showing predominantly spherical nanoparticles with strong silver signals and minor peaks of oxygen and carbon, indicative of biomolecular capping. Similar results reported in AgNPs synthesized from *Ocimum sanctum* reinforce the universal role of plant-derived compounds in nanoparticle stabilization [24].

The novelty of this study lies in employing *C. spectabilis*, a species rarely explored for nanomaterial synthesis, yet capable of generating nanoparticles with physicochemical properties comparable to those produced by widely studied medicinal plants. The small and uniform particle size observed suggests potential biomedical relevance, as smaller AgNPs typically exhibit enhanced antimicrobial activity owing to their higher surface area-to-volume ratio.

In conclusion, *C. spectabilis* leaf extract represents an effective and eco-friendly biogenic source for synthesizing stable, crystalline AgNPs. Compared with other plant-based systems, the nanoparticles produced in this study demonstrate competitive characteristics in terms of size, morphology, and stability, thereby offering a novel and sustainable route for applications in biomedical and environmental domains.

V. CONCLUSION

The present study successfully demonstrated the green synthesis of silver nanoparticles (AgNPs) using *Crotalaria spectabilis* leaf extract, which acted as both a reducing and stabilizing agent. EDX analysis confirmed the elemental composition with dominant silver peaks, validating the purity and successful biosynthesis of the nanoparticles. FTIR spectra revealed the involvement of phytochemicals such as phenols, flavonoids, proteins, and polysaccharides, indicating their dual role in reducing Ag^+ ions and stabilizing the nanoparticles through capping. SEM micrographs showed predominantly spherical nanoparticles with slight aggregation, a feature commonly observed in biogenically synthesized nanoparticles due to the association of surface biomolecules. XRD analysis further verified the crystalline nature of the AgNPs, displaying sharp diffraction peaks characteristic of the face-centered cubic (fcc) structure of silver, with estimated crystallite sizes in the range of 24.6 nm. Complementary GC–MS profiling of methanolic and ethanolic extracts revealed a variety of bioactive compounds, for example, terpenoids, phenolic derivatives, imidazoles, benzofuran derivatives, and siloxane compounds. These metabolites likely contributed to the reduction as well as stabilization processes, while also imparting potential biological activities to the synthesized nanoparticles. Overall, the study establishes *Crotalaria spectabilis* as a promising biogenic source for the eco-friendly synthesis of stable, crystalline, and nanosized AgNPs. By avoiding hazardous chemicals, phytochemical-assisted synthesis offers a sustainable approach to nanomaterial production. The biogenic AgNPs produced here hold significant potential for applications in antimicrobial development, agriculture, environmental remediation, and biomedical sciences.

ACKNOWLEDGEMENT

The author gratefully acknowledges the financial assistance received from the Council of Scientific and Industrial Research (CSIR), Government of India, in the form of a research fellowship.

CONFLICT OF INTEREST

All authors declare that they have no conflict of interest.

REFERENCES

[1] M. Ajaz, W. Rasool, and A. Mahmood, “Comprehensive review of nanotechnology: Innovations and multidisciplinary applications,” *Futur. Biotechnol.,* pp. 12–18, 2024.

[2] B. Asiyanbola and W. Soboyejo, “For the surgeon: An introduction to nanotechnology,” *J. Surg. Educ*., vol. 65, no. 2, pp. 155–161, Mar. 2008.

[3] B. Kumar, K. Smita, L. Cumbal, and A. Debut, “Green synthesis of silver nanoparticles using Andean blackberry fruit extract,” *Saudi J. Biol. Sci*., vol. 24, no. 1, pp. 45–50, 2017.

[4] D. Bharathi, M. D. Josebin, S. Vasantharaj, and V. Bhuvaneshwari, “Biosynthesis of silver nanoparticles using stem bark extracts of *Diospyros montana* and their antioxidant and antibacterial activities*,” J. Nanostruct. Chem.*, vol. 8, no. 1, pp. 83–92, 2018.

[5] K. K. Jain, “Nanomedicine: Application of nanobiotechnology in medical practice,” *Med. Princ. Pract.*, vol. 17, no. 2, pp. 89–101, 2008.

[6] A. Sati, S. N. Mali, T. N. Ranade, S. Yadav, and A. Pratap, “Silver nanoparticles (AgNPs) as a double-edged sword: Synthesis, factors affecting, mechanisms of toxicity and anticancer potentials—An updated review till March 2025,” *Biol. Trace Elem. Res*., pp. 1–52, 2025.

[7] S. S. Salem and A. Fouda, “Green synthesis of metallic nanoparticles and their prospective biotechnological applications: An overview,” *Biol. Trace Elem. Res*., vol. 199, no. 1, pp. 344–370, 2021.

[8] V. Duraipandiyan, M. Ayyanar, and S. Ignacimuthu, “Antimicrobial activity of some ethnomedicinal plants used by Paliyar tribe from Tamil Nadu, India,” BMC Complement. *Altern. Med.,* vol. 6, pp. 35–41, 2006.

[9] V. V. Makarov, A. J. Love, O. V. Sinitsyna, S. S. Makarova, I. V. Yaminsky, M. E. Taliansky, and N. O. Kalinina, “‘Green’ nanotechnologies: Synthesis of metal nanoparticles using plants,” *Acta Naturae*, vol. 6, no. 1(20), pp. 35–44, 2014.

[10] A. Verma, and M. S. Mehata, “Controllable synthesis of silver nanoparticles using Neem leaves and their antimicrobial activity,” *J. Radiat. Res. Appl. Sci.,* vol. 9, no. 1, pp. 109–115, 2016.

[11] A. R. Bhatlawande, P. U. Ghatge, G. U. Shinde, R. K. Anushree, and S. D. Patil, “Unlocking the future of smart food packaging: Biosensors, IoT, and nano materials,” *Food Sci. Biotechnol*., vol. 33, no. 5, pp. 1075–1091, 2024.

[12] O. R. Alara, N. H. Abdurahman, C. I. Ukaegbu, and N. A. Kabbashi, “Extraction and characterization of bioactive compounds in *Vernonia amygdalina* leaf ethanolic extract comparing Soxhlet and microwave-

assisted extraction techniques," *J. Taibah Univ. Sci.,* vol. 13, no. 1, pp. 414–422, 2019.

[13] M. Al-Owaisi, N. Al-Hadiwi, and S. A. Khan, "GC-MS analysis, determination of total phenolics, flavonoid content and free radical scavenging activities of various crude extracts of *Moringa peregrina* (Forssk.) Fiori leaves," *Asian Pac. J. Trop. Biomed*., vol. 4, no. 12, pp. 964–970, 2014.

[14] W. A. Carrick, D. B. Cooper, and B. Muir, "Retrospective identification of chemical warfare agents by high-temperature automatic thermal desorption–gas chromatography–mass spectrometry," *J. Chromatogr. A*, vol. 925, no. 1–2, pp. 241–249, 2001.

[15] P. Banerjee, M. Satapathy, A. Mukhopahayay, and P. Das, "Leaf extract mediated green synthesis of silver nanoparticles from widely available Indian plants: Synthesis, characterization, antimicrobial property and toxicity analysis," *Bioresour. Bioprocess*., vol. 1, no. 1, p. 3, 2014.

[16] C. Castiello, P. Junghanns, A. Mergel, C. Jacob, C. Ducho, S. Valente, and A. Mai, "GreenMedChem: The challenge in the next decade toward eco-friendly compounds and processes in drug design," *Green Chem*., vol. 25, no. 6, pp. 2109–2169, 2023.

[17] N. Bahari, N. Hashim, K. Abdan, A. Md Akim, B. Maringgal, and L. Al-Shdifat, "Role of honey as a bifunctional reducing and capping/stabilizing agent: Application for silver and zinc oxide nanoparticles," *Nanomaterials,* vol. 13, no. 7, p. 1244, 2023.

[18] B. K. Mehta, M. Chhajlani, and B. D. Shrivastava, "Green synthesis of silver nanoparticles and their characterization by XRD," *J. Phys.: Conf. Ser.*, vol. 836, no. 1, p. 012050, Apr. 2017.

[19] Ahmed Abdelmoteleb, Braulio Valdez-Salas, Cecilia Ceceña-Duran, Omar Tzintzun-Camacho, Francisco Gutiérrez-Miceli, Omar Grimaldo-Juarez, and Diana González-Mendoza, "Silver nanoparticles from *Prosopis glandulosa* and their potential application as biocontrol of *Acinetobacter calcoaceticus* and *Bacillus cereus*," *Chem. Speciation Bioavailab.*, vol. 29, no. 1, pp. 1–5, 2017.

[20] R. Sathyavathi, M. B. Krishna, S. V. Rao, R. Saritha, and D. N. Rao, "Biosynthesis of silver nanoparticles using *Coriandrum sativum* leaf extract and their application in nonlinear optics," *Adv. Sci. Lett.*, vol. 3, no. 2, pp. 138–143, 2010.

[21] M. A. J. Kouhbanani, N. Beheshtkhoo, P. Nasirmoghadas, S. Yazdanpanah, K. Zomorodianc, S. Taghizadeh, and A. M. Amani, "Green synthesis of spherical silver nanoparticles using *Ducrosia anethifolia* aqueous extract and its antibacterial activity," *J. Environ. Treat. Tech.*, vol. 7, no. 3, pp. 461–466, 2019.

[22] M. Ansari, S. Ahmed, M. T. Khan, N. A. Hamad, H. M. Ali, A. Abbasi, M. Q. Shah, A. H. Khan, and I. K. Jasim, "Evaluation of in vitro and in vivo antifungal activity of green synthesized silver nanoparticles against early blight in tomato," *Horticulturae*, vol. 9, no. 3, p. 369, 2023.

[23] S. A. Kumari, A. K. Patlolla, and P. Madhusudhanachary, "Biosynthesis of silver nanoparticles using *Moringa oleifera* and their antioxidant and anticancer effects in cell lines," *Micromachines*, vol. 13, no. 9, p. 1416, 2022.

[24] A. M. Alex, S. Subburaman, S. Chauhan, V. Ahuja, G. Abdi, M. A. Tarighat, R. R. Ebrahimzadeh, K. Vellingiri, V. K. Sahu, S. M. Ghaffari, and A. K. Sharma, "Green synthesis of silver nanoparticles prepared with *Ocimum* species and assessment of anticancer potential," *Sci. Rep.*, vol. 14, p. 11707, 2024.